

Reconstruction of Quadratic Curves in 3-D from Two or More Perspective Views

R. BALASUBRAMANIAN^{a,*}, SUKHENDU DAS^{b,†} and K. SWAMINATHAN^{a,‡}

^a*Department of Mathematics,* ^b*Department of Computer Science and Engineering, Indian Institute of Technology, Madras, Chennai 600 036, India*

(Received 26 June 2001; In final form 28 August 2001)

The issues involved in the reconstruction of a quadratic curve in 3-D space from arbitrary perspective projections are described in this paper. Correspondence between the projections of the curve on the image planes is assumed to be established. Equations for reconstruction of the 3-D curve, which give the parameters of the 3-D quadratic curve are determined. Uniqueness of the solution in the process of reconstruction is addressed and solved using additional constraints. As practical examples, reconstruction of circles, parabolas and pair of straight lines in 3-D space are demonstrated.

Key words: Reconstruction, Quadratic curves, Perspective projections, Additional constraints

1 INTRODUCTION

Most natural as well as man-made objects have curved lines and surfaces. Reconstruction of curved lines of 3-D objects is an important task in many applications of Computer Vision such as estimation of 3-D object structure, object recognition and reconstruction. For objects with planar shapes, straight lines and points are used as features for reconstruction. This is not useful for objects with curved surfaces.

For objects with curved surfaces, the intersection of two surfaces (3-D edge) is a curve. Quadratic curves [5] which can represent a wide variety of curves in 3-D are used in this work. Projection of these curves onto image planes under perspective transformation produce conics. Two or more corresponding conics, from as many views, are used to reconstruct a curve in 3-D. The case of reconstruction of conics in 3-D space has been discussed by several authors in their work, [6–8, 10–12]. Though Xie and Thonnat in Ref. [11] give the analytical formulation for the reconstruction of quadratic curves, they have not given any methodology to determine the unique solution from the roots of a quadratic equation. In the case of planar curves, they have assumed the existence of a point to point correspondence between the sets of contour points on the pair of projected curve segments. Xie in Ref. [12] uses the planarity constraint and formulations given in Ref. [11] to obtain the unique solution in case of conics using point to point correspondence and has described a method to improve the quality of 3-D data related to quadratic curves. Quan in Ref. [18] has solved correspondence in the case of conics from two views. He has solved the ambiguity (non-uniqueness) in the solutions

* E-mail: balaiitm@yahoo.com

† E-mail: sdas@iitm.ac.in

‡Corresponding author. Fax: 044-2578470; E-mail: kswamy@iitm.ac.in

with the use of a non-transparency constraint of a conic section. Kanatani *et al.* in Ref. [6] have developed computation procedures to interpret the 3-D geometry of conics in the scene from their projections by giving real examples.

The work presented in this paper deals with the methodology of reconstruction of a quadratic curve in 3-D space from two or more arbitrary perspective views. Equations of reconstruction are presented, along with the examples from simulation studies. The issue of uniqueness of the solution is addressed and solved with the use of additional constraints.

2 FORMULATION OF THE PROBLEM

The imaging set-up using two cameras is shown in Figure 1. Let I_1 and I_2 be the first and second image planes of the pair of cameras C_1 and C_2 respectively. Let the position and the orientation of one camera be known with respect to another and both have a common field of view. Let O_1xyz be the rectangular cartesian frame of reference with its origin O_1 at the center of projection of one of the cameras C_1 . A point W in 3-D space, with co-ordinates

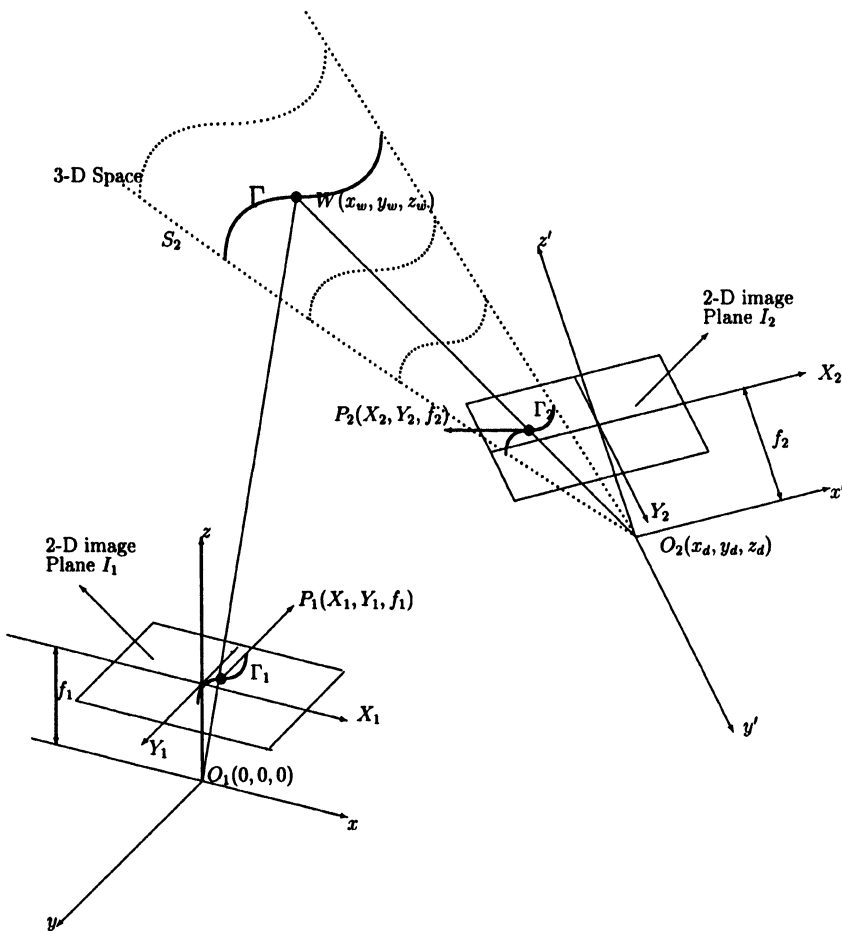


FIGURE 1 Reconstruction of a 3-D curve Γ from its pair of projections Γ_1 and Γ_2 on the image planes I_1 and I_2 respectively.

(x_w, y_w, z_w) with respect to the frame of reference at C_1 , is viewed by both the cameras C_1 and C_2 . Let $O_2x'y'z'$ be the second rectangular cartesian co-ordinate system, not necessarily parallel to $OXYZ$ system, with its origin O_2 at the center of projection of the second camera C_2 . Let the co-ordinates of the second camera C_2 with respect to O_1 be (x_d, y_d, z_d) . Let $P_1(X_1, Y_1, f_1)$ and $P_2(X_2, Y_2, f_2)$ be the corresponding pair of projections of point W on the pair of image planes I_1 and I_2 respectively. Let f_1 and f_2 be the focal lengths of the first and the second cameras respectively. The collinearity equations represent the mathematical process of image formation, linking the co-ordinates of a point on an object in 3-D space to the corresponding co-ordinates of its projection in the 2-D image plane. The collinearity equations are derived using the criteria that all the three points, namely, the center of perspective projection, the image point and the object point lie on the same straight line. Let the perspective projections of a quadratic curve Γ in 3-D space be a pair of quadratic curves Γ_1 and Γ_2 , on the first and second image planes respectively as shown in Figure 1. The problem is to reconstruct the 3-D quadratic curve Γ from the pair of its images Γ_1 and Γ_2 . The relation between the coordinates of the point $W(x_w, y_w, z_w)$ and that of the image point $P_1(X_1, Y_1, f_1)$ is given by the perspective equation [3, 4]:

$$X_1 = f_1 \frac{x_w}{z_w}, \quad Y_1 = f_1 \frac{y_w}{z_w} \tag{1}$$

The 3-D co-ordinates of point $W(x_w, y_w, z_w)$ with respect to second camera C_2 , is given by

$$\begin{bmatrix} x'_w \\ y'_w \\ z'_w \end{bmatrix} = \lambda \begin{bmatrix} \cos \alpha_1 & \cos \beta_1 & \cos \gamma_1 \\ \cos \alpha_2 & \cos \beta_2 & \cos \gamma_2 \\ \cos \alpha_3 & \cos \beta_3 & \cos \gamma_3 \end{bmatrix} \begin{bmatrix} (x_w - x_d) \\ (y_w - y_d) \\ (z_w - z_d) \end{bmatrix}, \tag{2}$$

where

$$\begin{aligned} \cos \alpha_1 &= \cos \psi \cos \phi - \cos \theta \sin \phi \sin \psi, \\ \cos \alpha_2 &= \cos \psi \sin \phi + \cos \theta \cos \phi \sin \psi, \\ \cos \alpha_3 &= \sin \psi \sin \theta, \\ \cos \beta_1 &= -\sin \psi \cos \phi - \cos \theta \sin \phi \cos \psi, \\ \cos \beta_2 &= -\sin \psi \sin \phi + \cos \theta \cos \phi \cos \psi, \\ \cos \beta_3 &= \cos \psi \sin \theta, \\ \cos \gamma_1 &= \sin \phi \sin \theta, \\ \cos \gamma_2 &= -\sin \theta \cos \phi, \\ \cos \gamma_3 &= \cos \theta, \end{aligned}$$

and θ, ϕ and ψ are the Eulerian angles.

In the above equations $\alpha_i, \beta_i, \gamma_i, (i = 1, 2, 3)$ are the respective direction cosines of the axes of $O_2x'y'z'$ with respect to O_1xyz system. λ is a scale factor between the two reference frames and without loss of generality this is considered to be 1, in this work. Using Eq. (2), the relation between the object space point $W(x_w, y_w, z_w)$ and the image point $P_2(X_2, Y_2, f_2)$ is given by the perspective equations [3, 4]:

$$X_2 = f_2 \frac{(x_w - x_d) \cos \alpha_1 + (y_w - y_d) \cos \beta_1 + (z_w - z_d) \cos \gamma_1}{(x_w - x_d) \cos \alpha_3 + (y_w - y_d) \cos \beta_3 + (z_w - z_d) \cos \gamma_3} \tag{3}$$

$$Y_2 = f_2 \frac{(x_w - x_d) \cos \alpha_2 + (y_w - y_d) \cos \beta_2 + (z_w - z_d) \cos \gamma_2}{(x_w - x_d) \cos \alpha_3 + (y_w - y_d) \cos \beta_3 + (z_w - z_d) \cos \gamma_3} \tag{4}$$

Equations (1), (3) and (4) are the collinearity equations for a pair of arbitrary perspective views [3, 4]. The method presented in this paper is similar to the work of Ref. [11, 12].

Xie and Thonnat [11] have addressed the problem of 3-D reconstruction of heterogeneous edge primitives by using two perspective views. They have illustrated the existence of analytical solutions with respect to the edge primitives like contour points, line segments, quadratic curves and closed curves. They derive their proposed solutions by reasoning in discrete space time. Hence they can be directly applied to the situation where a set of discrete digital images are available. However their analytical formulation for the reconstruction of quadratic curves does not give any methodology to determine the unique solution from the roots of the resulting quadratic equation.

Precision is the central issue in 3-D reconstruction. In order to find solution to this problem, most of the efforts have been dedicated to the approaches of fusion. Xie [12] has shown that the quality of 3-D reconstruction can be improved by carefully choosing a reconstruction strategy. Xie also has demonstrated experimentally the usefulness of his solution for the 3-D reconstruction of quadratic curves. He uses the planarity constraint and formulations given in Ref. [11] to obtain the unique solution in case of conics using point to point correspondence and has given a method to improve the quality of 3-D data related to quadratic curves.

Quan in Ref. [8] has solved correspondence in the case of conics from two views. He has shown that there are two independent polynomial conditions on the corresponding pairs of conics across two views, given the relative orientation of the two views. He has derived these two correspondence conditions algebraically and shown one of them to be fundamental in establishing the correspondence of conics. He has solved the ambiguity (non-uniqueness) in the solutions with the use of a non-transparency constraint of a conic section.

All the methodologies developed by various research workers to reconstruct a conic is based on point to point correspondence. The corresponding analytical formulations for the reconstruction of quadratic curves or conics do not give any methodology to determine the unique solution from the roots of the resulting quadratic equation. But in the work described here, point to point correspondence between contours of projected curved segments has not been assumed and a methodology to determine the unique solution is given. Although use of planarity constraint has been made as given by Xie *et al.* [11], the method proposed in this paper is applicable for the reconstruction of wired and transparent conical sections. It is also shown that a third view is necessary in a particular case to obtain the unique solution. Quadratic curves in this paper mean the curves whose projections onto the image planes, that can be described by an equation of quadratic form.

3 RECONSTRUCTION METHODOLOGY

In this problem, least square regression is used to obtain the parameters of the 2-D quadratic curves Γ_1 and Γ_2 . Let the equations of the conics $\Gamma_j, j = 1, 2$ in the respective pair of image planes I_1 and I_2 be given by

$$A_{vj}X_{vj}^2 + B_{vj}Y_{vj}^2 + C_{vj}X_{vj}Y_{vj} + E_{vj}X_{vj} + F_{vj}Y_{vj} + G_{vj} = 0, \quad j = 1, 2.$$

Consider a quadratic surface S_2 which passes through the centre of projection of the second camera O_2 and the projected quadratic curve Γ_2 . Surface S_2 is represented as a non-linear function of a set of parameters of the curve Γ_2 and geometry of the imaging setup. Choose

any point $P_1(X_1, Y_1)$ on the curve Γ_1 in the first image plane. The equation of the line O_1P_1 , joining the centre of projection of the first camera O_1 and point P_1 , is given by

$$\frac{x}{X_1} = \frac{y}{Y_1} = \frac{z}{f_1} = r, \quad (5)$$

where without loss of generality, f_1 is chosen to be unity. Intersection of line O_1P_1 with surface S_2 is obtained as follows:

Let the equation of the curve Γ_1 in the first image plane I_1 be

$$A_{v1} X_{v1}^2 + B_{v1} Y_{v1}^2 + C_{v1} X_{v1} Y_{v1} + E_{v1} X_{v1} + F_{v1} Y_{v1} + G_{v1} = 0, \quad (6)$$

and the equation of the corresponding curve Γ_2 on the second image plane I_2 be,

$$A_{v2} X_{v2}^2 + B_{v2} Y_{v2}^2 + C_{v2} X_{v2} Y_{v2} + E_{v2} X_{v2} + F_{v2} Y_{v2} + G_{v2} = 0, \quad (7)$$

Since (X_2, Y_2) is a point on the curve Γ_2 , using the collinearity equations (1)–(4), the above Eq. (7) reduces to

$$A_{v2} \left\{ \frac{x'_w}{z'_w} \right\}^2 + B_{v2} \left\{ \frac{y'_w}{z'_w} \right\}^2 + C_{v2} \left\{ \frac{x'_w}{z'_w} \right\} \left\{ \frac{y'_w}{z'_w} \right\} + E_{v2} \left\{ \frac{x'_w}{z'_w} \right\} + F_{v2} \left\{ \frac{y'_w}{z'_w} \right\} + G_{v2} = 0$$

or

$$A_{v2} x_w'^2 + B_{v2} y_w'^2 + C_{v2} x_w' y_w' + E_{v2} x_w' z_w' + F_{v2} y_w' z_w' + G_{v2} z_w'^2 = 0 \quad (8)$$

where (x'_w, y'_w, z'_w) is the object point W in 3-D space with respect to the second camera system $O_2(x_d, y_d, z_d)$. With respect to $O_1(0, 0, 0)$ the above equation can be written as

$$\begin{aligned} & A_{v2} [(x_w - x_d) \cos \alpha_1 + (y_w - y_d) \cos \beta_1 + (z_w - z_d) \cos \gamma_1]^2 \\ & + B_{v2} [(x_w - x_d) \cos \alpha_2 + (y_w - y_d) \cos \beta_2 + (z_w - z_d) \cos \gamma_2]^2 \\ & + C_{v2} [(x_w - x_d) \cos \alpha_1 + (y_w - y_d) \cos \beta_1 + (z_w - z_d) \cos \gamma_1] \\ & \times [(x_w - x_d) \cos \alpha_2 + (y_w - y_d) \cos \beta_2 + (z_w - z_d) \cos \gamma_2] \\ & + E_{v2} [(x_w - x_d) \cos \alpha_1 + (y_w - y_d) \cos \beta_1 + (z_w - z_d) \cos \gamma_1] \\ & \times [(x_w - x_d) \cos \alpha_3 + (y_w - y_d) \cos \beta_3 + (z_w - z_d) \cos \gamma_3] \\ & + F_{v2} [(x_w - x_d) \cos \alpha_2 + (y_w - y_d) \cos \beta_2 + (z_w - z_d) \cos \gamma_2] \\ & \times [(x_w - x_d) \cos \alpha_3 + (y_w - y_d) \cos \beta_3 + (z_w - z_d) \cos \gamma_3] \\ & + G_{v2} [(x_w - x_d) \cos \alpha_3 + (y_w - y_d) \cos \beta_3 + (z_w - z_d) \cos \gamma_3]^2 = 0 \end{aligned} \quad (9)$$

Let

$$x_d \cos \alpha_k + y_d \cos \beta_k + z_d \cos \gamma_k = A_{\alpha_k}$$

for $k = 1, 2$ and 3 , then the above Eq. (5) becomes,

$$A_1x_w^2 + A_2y_w^2 + A_3z_w^2 + A_4x_wy_w + A_5y_wz_w + A_6z_wx_w + A_7x_w + A_8y_w + A_9z_w + A_{10} = 0 \quad (10)$$

which represents the equation of the surface S_2 , where

$$\begin{aligned} A_1 &= A_{v2} \cos^2 \alpha_1 + B_{v2} \cos^2 \alpha_2 + C_{v2} \cos \alpha_1 \alpha_2 + E_{v2} \cos \alpha_1 \alpha_3 + F_{v2} \cos \alpha_2 \cos \alpha_3 \\ &\quad + G_{v2} \cos^2 \alpha_3 \\ A_2 &= A_{v2} \cos^2 \beta_1 + B_{v2} \cos^2 \beta_2 + C_{v2} \cos \beta_1 \beta_2 + E_{v2} \cos \beta_1 \beta_3 + F_{v2} \cos \beta_2 \cos \beta_3 \\ &\quad + G_{v2} \cos^2 \beta_3 \\ A_3 &= A_{v2} \cos^2 \gamma_1 + B_{v2} \cos^2 \gamma_2 + C_{v2} \cos \gamma_1 \gamma_2 + E_{v2} \cos \gamma_1 \gamma_3 + F_{v2} \cos \gamma_2 \cos \gamma_3 + G_{v2} \cos^2 \gamma_3 \\ A_4 &= 2A_{v2} \cos \alpha_1 \cos \beta_1 + 2B_{v2} \cos \alpha_2 \cos \beta_2 + C_{v2}(\cos \alpha_1 \cos \beta_2 + \cos \alpha_2 \cos \beta_1) \\ &\quad + E_{v2}(\cos \alpha_1 \cos \beta_3 + \cos \alpha_3 \cos \beta_1) + F_{v2}(\cos \alpha_2 \cos \beta_3 + \alpha_3 \beta_2) + 2G_{v2} \cos \alpha_3 \cos \beta_3 \\ A_5 &= 2A_{v2} \cos \gamma_1 \cos \beta_1 + 2B_{v2} \cos \gamma_2 \cos \beta_2 + C_{v2}(\cos \gamma_2 \cos \beta_1 + \cos \gamma_1 \cos \beta_2) \\ &\quad + E_{v2}(\cos \beta_1 \cos \gamma_3 + \cos \beta_3 \cos \gamma_1) + F_{v2}(\cos \beta_2 \cos \gamma_3 + \cos \beta_3 \cos \gamma_2) \\ &\quad + 2G_{v2} \cos \beta_3 \cos \gamma_3 \\ A_6 &= 2A_{v2} \cos \gamma_1 \cos \alpha_1 + 2B_{v2} \cos \gamma_2 \cos \alpha_2 + C_{v2}(\cos \gamma_1 \cos \alpha_2 + \cos \gamma_2 \cos \alpha_1) \\ &\quad + E_{v2}(\cos \gamma_1 \cos \alpha_3 + \cos \gamma_3 \cos \alpha_1) + F_{v2}(\cos \gamma_2 \cos \alpha_3 + \cos \gamma_3 \cos \alpha_2) \\ &\quad + 2G_{v2} \cos \gamma_3 \cos \alpha_3 \\ A_7 &= -\{2A_{v2}A_{\alpha_1} \cos \alpha_1 + 2B_{v2}A_{\alpha_2} \cos \alpha_2 + C_{v2}(\cos \alpha_1 A_{\alpha_2} + \cos \alpha_2 A_{\alpha_1}) \\ &\quad + E_{v2}(\cos \alpha_1 A_{\alpha_3} + \cos \alpha_3 A_{\alpha_1}) + F_{v2}(\cos \alpha_2 A_{\alpha_3} + \cos \alpha_3 A_{\alpha_2} + 2G_{v2}A_{\alpha_3} \cos \alpha_3)\} \\ A_8 &= -(2A_{v2}A_{\alpha_1} \cos \beta_1 + 2B_{v2}A_{\alpha_2} \cos \beta_2 + C_{v2}(\cos \beta_1 A_{\alpha_2} + \cos \beta_2 A_{\alpha_1}) \\ &\quad + E_{v2}(\cos \beta_1 A_{\alpha_3} + \cos \beta_3 A_{\alpha_1}) + F_{v2}(\cos \beta_2 A_{\alpha_3} + \cos \beta_3 A_{\alpha_2} + 2G_{v2}(A_{\alpha_3} \cos \beta_3)) \\ A_9 &= -(2A_{v2}A_{\alpha_1} \cos \gamma_1 + 2B_{v2}A_{\alpha_2} \cos \gamma_2 + C_{v2}(\cos \gamma_1 A_{\alpha_2} + \cos \gamma_2 A_{\alpha_1}) \\ &\quad + E_{v2}(\cos \gamma_1 A_{\alpha_3} + \cos \gamma_3 A_{\alpha_1}) + F_{v2}(\cos \gamma_2 A_{\alpha_3} + \cos \gamma_3 A_{\alpha_2} + 2G_{v2}(A_{\alpha_3} \cos \gamma_3)) \\ A_{10} &= A_{v2}A_{\alpha_1}^2 + B_{v2}A_{\alpha_2}^2 + C_{v2}A_{\alpha_1}A_{\alpha_2} + E_{v2}A_{\alpha_1}A_{\alpha_3} + F_{v2}A_{\alpha_2}A_{\alpha_3} + G_{v2}A_{\alpha_3}^2 \end{aligned}$$

Now the equation of the line O_1P_1 is given by

$$\frac{x}{X_1} = \frac{y}{Y_1} = \frac{z}{f_1} = r \quad (11)$$

Hence,

$$\begin{aligned} x &= rX_1 \\ y &= rY_1 \\ z &= rf_1 \end{aligned}$$

Thus this reduces to a problem of finding the point of intersection of the surface S_2 and a line O_1P_1 , since we are considering $f_1 = 1$, the Eq. (10) becomes

$$(A_1X_1^2 + A_2Y_1^2 + A_3 + A_4X_1Y_1 + A_5Y_1 + A_6X_1)r^2 + (A_7X_1 + A_8Y_1 + A_9)r + A_{10} = 0 \tag{12}$$

Denoting

$$\begin{aligned} a &= A_1X_1^2 + A_2Y_1^2 + A_3 + A_4X_1Y_1 + A_5Y_1 + A_6X_1 \\ b &= A_7X_1 + A_8Y_1 + A_9 \\ c &= A_{10}, \end{aligned}$$

the above equation can be rewritten as,

$$ar^2 + br + c = 0 \tag{13}$$

It can be seen that a , b and c are functions of (i) parameters of the second conic ($A_{v2}, B_{v2}, C_{v2}, E_{v2}, F_{v2}, G_{v2}$), (ii) orientation parameters of the second camera system ($\cos \alpha_1, \cos \beta_1, \cos \gamma_1, \cos \alpha_2, \cos \beta_2, \cos \gamma_2, \cos \alpha_3, \cos \beta_3, \cos \gamma_3$) and (iii) position (x_d, y_d, z_d) of the second camera. The co-ordinates of the points of intersection of line O_1P_1 and surface S_2 in 3-D space, are given in terms of the solution r of Eqs. (11) and (13) as:

$$z = \frac{-b \pm \sqrt{(b^2 - 4ac)}}{2a}, \quad x = z X_1, \quad y = z Y_1 \tag{14}$$

Choose a set of N contour points $P_{i1}(X_i, Y_i)$, $i = 1, 2, \dots, N$, on the curve Γ_1 in the first image plane. Using (14), two sets of coordinate values (x_{i1}, y_{i1}, z_{i1}) and (x_{i2}, y_{i2}, z_{i2}) , $i = 1, 2, \dots, N$, are obtained, where N is the number of discrete data points P_{i1} on curve Γ_1 . Hence this gives two sets of depth values of the points as candidates for the solution. Let z_{i1} and z_{i2} , $i = 1, 2, \dots, N$, be the pair of sequence of depth values of a set of potential candidate points obtained for the reconstruction of the 3-D curve Γ , which are given as

$$\begin{aligned} z_{i1} &= \frac{-b + \sqrt{(b^2 - 4ac)}}{2a}, & x_{i1} &= z_{i1} X_i, & y_{i1} &= z_{i1} Y_i \\ z_{i2} &= \frac{-b - \sqrt{(b^2 - 4ac)}}{2a}, & x_{i2} &= z_{i2} X_i, & y_{i2} &= z_{i2} Y_i \end{aligned}$$

Assuming r to be positive (which is a constraint from the geometry of the imaging setup), only positive values of z_{i1} and z_{i2} are acceptable. Two cases arise from the solution given in Eq. (14), and correspondingly the methods to obtain the unique solution for reconstruction of the 3-D curve are described in the next section.

4 SIMULATION RESULTS FOR DIFFERENT CURVES

Case I Some of the solutions are negative, (i.e., for some i , say, $z_{i1} \leq 0$ and $z_{i2} > 0$).

Figures 2(a), 7(a) and 10(a) show the typical plots of pair of sequences of depth values of candidate points for reconstruction of circles, parabolas and pair of straight lines in 3-D

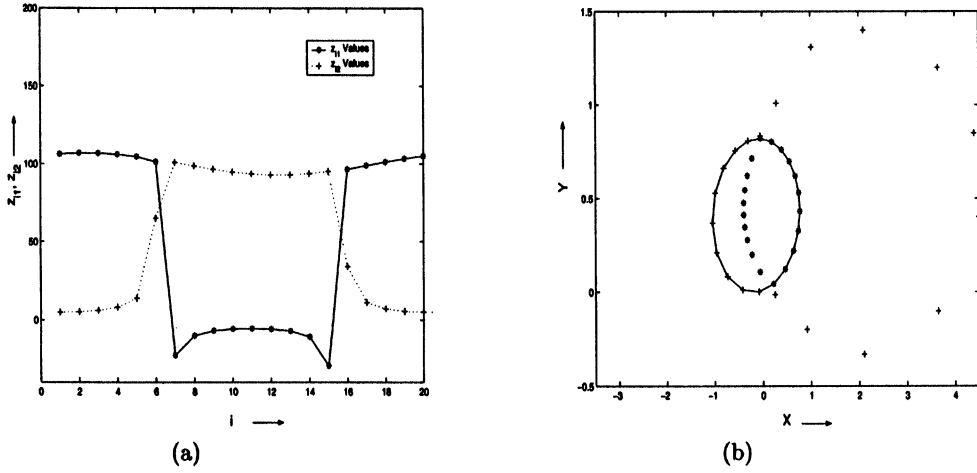


FIGURE 2 (a) Plot of pair of sequence of z values obtained for the reconstruction of a circle in 3-D space using perfect stereo. Equation of the circle is: $x = 40 + 99.6195 \cos t - 3.1751 \sin t$, $y = 70 + 5.9696 \cos t + 49.80975 \sin t$ and $z = 100 + 6.3502 \cos t + 2.9848 \sin t$, $0 \leq t \leq 2\pi$, $x_d = 10.0$, $y_d = 0.0$, $z_d = 0.0$. (b) Reconstruction of a circle for the data used in Figure 2(a) using a third projection. The projection of the pair of sequences obtained as solutions in Figure 2(a) are superimposed on the projection of the circle. This helps to identify the unique solution among the two possible solutions.

respectively. Select only those pair of solutions which have one negative value. Choose the corresponding positive value from only these selected set of pairs as the unique solution for curve Γ . Use these points to obtain the equation of the supporting plane of the curve Γ . Use the equation of the plane to identify the points actually lying on the curve (planarity constraint). Regress on the set of points identified as unique solutions to obtain the parameters of

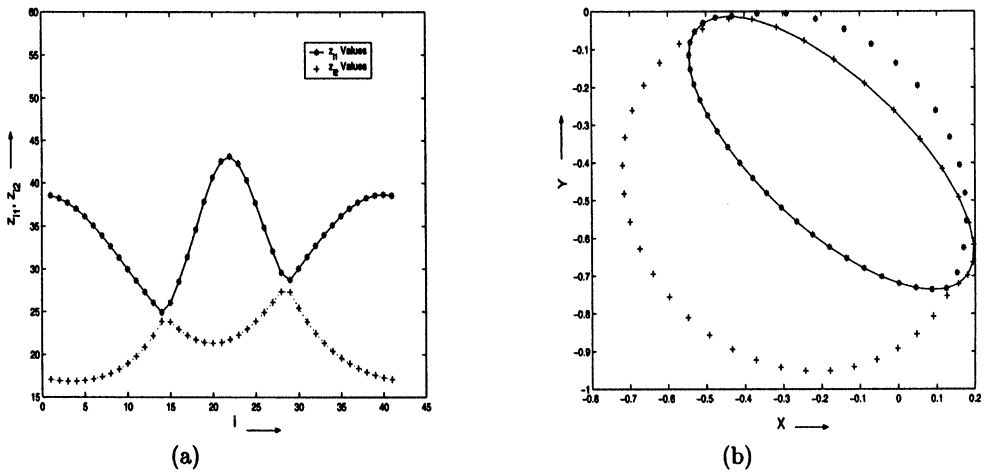


FIGURE 3 (a) Plot of pair of sequence of z values obtained for the reconstruction of a circle in 3-D space using general case. Equation of the circle is: $x = -5 \cos t - 4.80141 \sin t$, $y = -1.39516 \cos t + 8.66025 \sin t$ and $z = 30 + 8.54714 \cos t - 1.39516 \sin t$, $0 \leq t \leq 2\pi$, $x_d = 70.0$, $y_d = 10.0$, $z_d = 60.0$ and $\alpha_1 = 120^\circ$, $\beta_2 = 30^\circ$, $\gamma_3 = 120^\circ$. (b) Reconstruction of a circle for the data used in Figure 3(a) using a third projection. The projection of the pair of sequences obtained as solutions in Figure 3(a) are superimposed on the third projection of the circle. This helps to identify the unique solution among the two possible solutions.

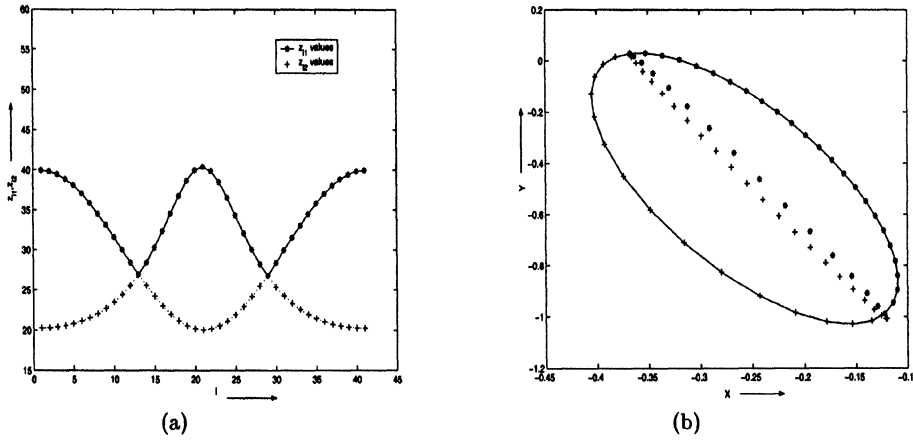


FIGURE 4 (a) Plot of pair of sequence of z values obtained for the reconstruction of a circle in 3-D space using general case. Equation of the circle is: $x = 0.87156 \cos t - 0.87072 \sin t$, $y = -0.03809 \cos t + 9.96195 \sin t$ and $z = 30 + 9.96187 \cos t + 0.03809 \sin t$, $0 \leq t \leq 2\pi$, $x_d = 60$, $y_d = 0$, $z_d = 30$, $\alpha_1 = 85^\circ$, $\beta_2 = 5^\circ$, $\gamma_3 = 85^\circ$. (b) Reconstruction of a circle for the data used in Figure 4(a) using a third projection. The projection of the pair of sequences obtained as solutions in Figure 4(a) are superimposed on the third projection of the circle. This helps to identify the unique solution among the two possible solutions.

the quadratic equation representing the curve Γ . Figures 2(b), 7(b) and 10(b) illustrate a suitable projection of the pair of sequences for the data given in Figures 2(a), 7(a) and 10(a), where the unique solution is shown as a continuous curve.

Case II All the solutions are positive.

To eliminate the ambiguity and provide a unique solution we need an additional constraint. For using the planarity constraint of Xie *et al.*, [11], point to point correspondence is

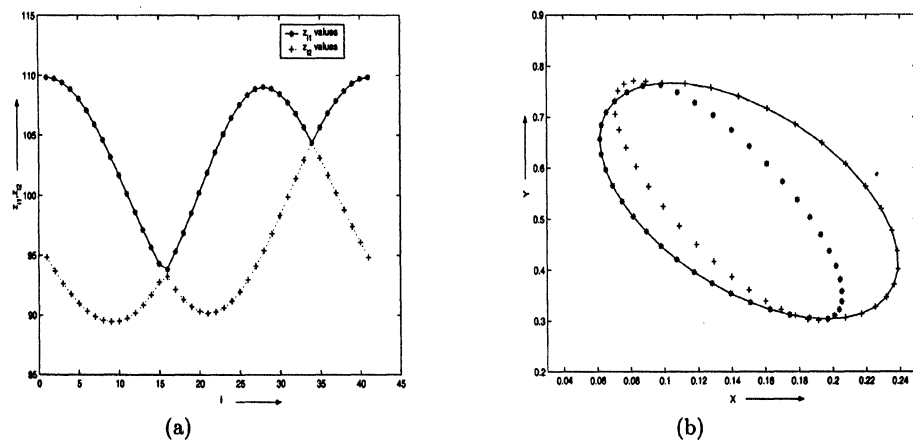


FIGURE 5 (a) Plot of pair of sequence of z values obtained for the reconstruction of a circle in 3-D space using general case. Equation of the circle is: $x = 40 + 1.73648 \cos t - 1.72977 \sin t$, $y = 70 + 0.15251 \cos t + 9.84808 \sin t$ and $z = 100 + 9.84690 \cos t - 0.15251 \sin t$, $0 \leq t \leq 2\pi$, $x_d = 100$, $y_d = 70$, $z_d = 100$, $\alpha_1 = 80^\circ$, $\beta_2 = 10^\circ$, $\gamma_3 = 80^\circ$. (b) Reconstruction of a circle for the data used in Figure 5(a) using a third projection. The projection of the pair of sequences obtained as solutions in Figure 5(a) are superimposed on the third projection of the circle. This helps to identify the unique solution among the two possible solutions.

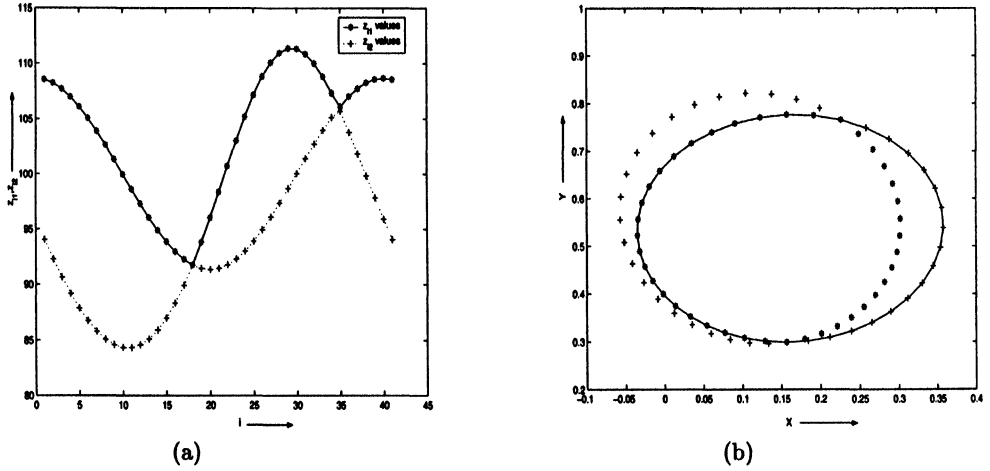


FIGURE 6 (a) Plot of pair of sequence of z values obtained for the reconstruction of a circle in 3-D space using general case. Equation of the circle is: $x = 40 - 5 \cos t - 4.80141 \sin t$, $y = 70 - 1.39516 \cos t + 8.66025 \sin t$ and $z = 30 + 8.54714 \cos t - 1.39516 \sin t$, $0 \leq t \leq 2\pi$, $x_d = 100$, $y_d = 70$, $z_d = 120$, $\alpha_1 = 120^\circ$, $\beta_2 = 30^\circ$, $\gamma_3 = 120^\circ$. (b) Reconstruction of a circle for the data used in Figure 6(a) using a third projection. The projection of the pair of sequences obtained as solutions in Figure 6(a) are superimposed on the third projection of the circle. This helps to identify the unique solution among the two possible solutions.

necessary. Transparency constraint could be used to eliminate the ambiguity for solid (opaque) objects, [8]. For a more general case, if the curve/conic is wired or transparent, unique solution is possible only with the help of a third view, which identifies the unique solution. Figures 3(a), 4(a), 5(a) and 6(a) show plots of such a pair of sequences for the

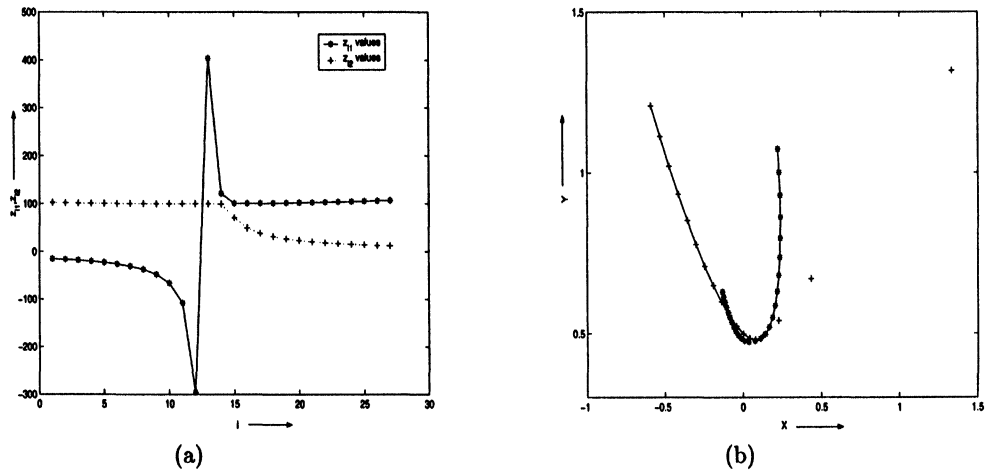


FIGURE 7 (a) Plot of pair of sequence of z values obtained for the reconstruction of a parabola in 3-D space using perfect stereo case. Equation of the parabola is: $x = 40 + 9.96195t - 0.31751t^2$, $y = 70 + 0.59696t + 4.980975t^2$ and $z = 100 + 0.63502t + 0.29848t^2$, $-4 \leq t \leq 4$, $x_d = 10$, $y_d = 0$, $z_d = 0$. (b) Reconstruction of a parabola for the data used in Figure 7(a) using a third projection. The projection of the pair of sequences obtained as solutions in Figure 7(a) are superimposed on the third projection of the parabola. This helps to identify the unique solution among the two possible solutions.

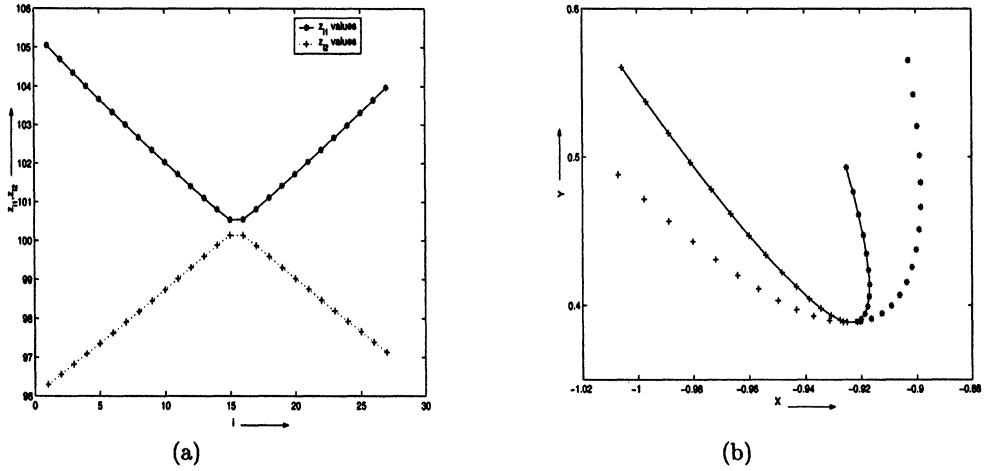


FIGURE 8 (a) Plot of pair of sequence of z values obtained for the reconstruction of a parabola in 3-D space using general case. Equation of the parabola is: $x = 40 + 0.173648t - 0.172977t^2$, $y = 70 + 0.015251t + 0.984808t^2$ and $z = 100 + 0.984690t + 0.015251t^2$, $-4 \leq t \leq 4$, $x_d = 100$, $y_d = 70$, $z_d = 100$, $\alpha_1 = 80^\circ$, $\beta_2 = 10^\circ$, $\gamma_3 = 80^\circ$. (b) Reconstruction of a parabola for the data used in Figure 8(a) using a third projection. The projection of the pair of sequences obtained as solutions in Figure 8(a) are superimposed on the third projection of the parabola. This helps to identify the unique solution among the two possible solutions.

reconstruction of different circles, for which the respective third view is shown in Figures 3(b), 4(b), 5(b) and 6(b). The projection of the circle obtained from this additional (third) view identifies the unique solution. Similarly the case of parabolas is shown in the Figures 8(a) and 8(b) and the case of pair of straight lines is shown in the Figures 9 and 11.

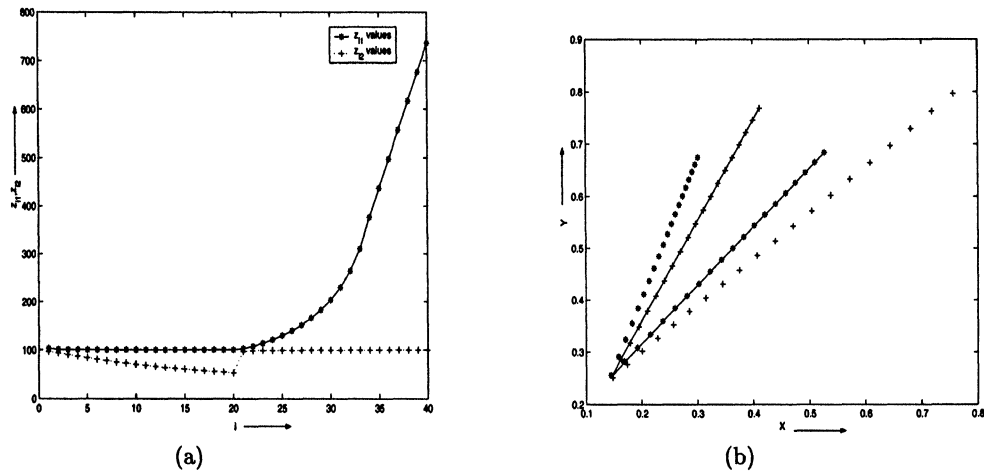


FIGURE 9 (a) Plot of pair of sequence of z values obtained for the reconstruction of a pair of straight lines in 3-D space using perfect stereo case. Equations of the pair of straight lines are: $x = 40 + 50t$, $y = 50 + 40t$ and $z = 100$, $x = 40 + 40t_1$, $y = 50 + 50t_1$ and $z = 100$, $0 \leq t, t_1 \leq 1.0$, $x_d = 20.0$, $y_d = 0.0$, $z_d = 0.0$. (b) Reconstruction of a pair of straight lines for the data used in Figure 9(a) using a third projection. The projection of the pair of sequences obtained as solutions in Figure 9(a) are superimposed on the third projection of the pair of straight lines. This helps to identify the unique solution among the possible solutions.

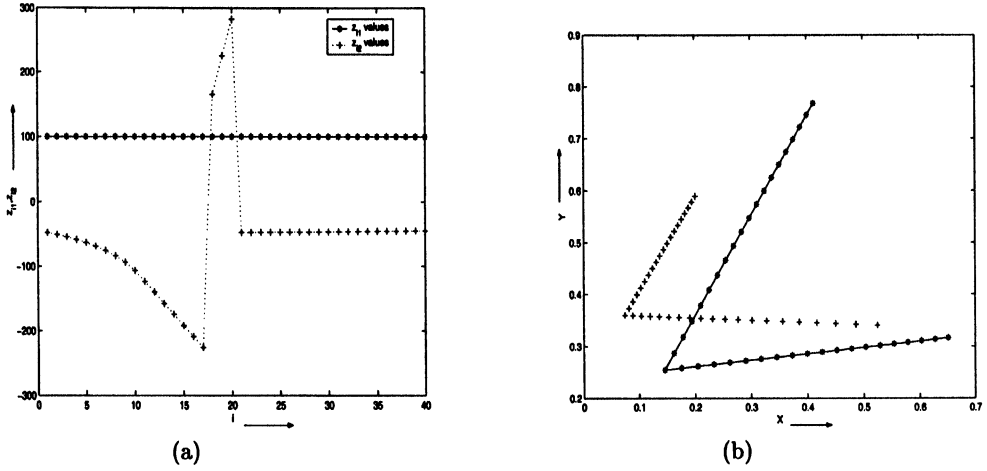


FIGURE 10 (a) Plot of pair of sequence of z values obtained for the reconstruction of a pair of straight lines in 3-D space using general case. Equations of the pair of straight lines are: $x = 40 + 50t, y = 50$ and $z = 100, x = 40 + 40t, y = 50 + 50t$ and $z = 100, 0 \leq t, t_1 \leq 1.0, x_d = 100.0, y_d = 50.0, z_d = 100.0, \alpha_1 = 80^\circ, \beta_2 = 10^\circ, \gamma_3 = 80^\circ$. (b) Reconstruction of a pair of straight lines for the data used in Figure 10(a) using a third projection. The projection of the pair of sequences obtained as solutions in Figure 10(a) are superimposed on the third projection of the pair of straight lines. This helps to identify the unique solution among the two possible solutions.

Using the constraint of continuity or smoothness of the curve, the two possible solutions are classified. If the surface enclosed by the curve is opaque, only one of the solutions will be visible. In the case of transparent structures or wired conics, a third view is mandatory.

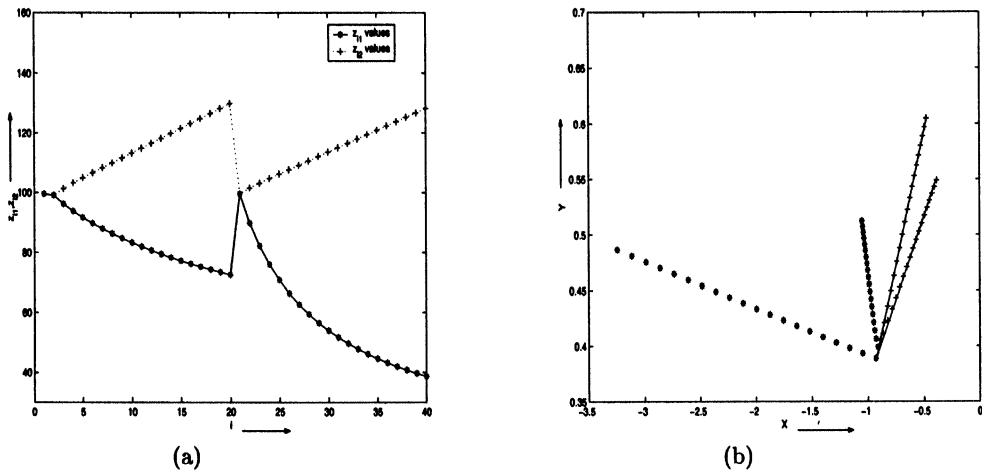


FIGURE 11 (a) Plot of pair of sequence of z values obtained for the reconstruction of a pair of straight lines in 3-D space using general case. Equations of the pair of straight lines are: $x = 40 + 50t, y = 70 + 40t$ and $z = 100 + 30t, x = 40 + 40t_1, y = 70 + 50t_1$ and $z = 100 + 30t_1, 0 \leq t, t_1 \leq 1.0, x_d = 70.0, y_d = 70.0, z_d = 60.0, \alpha_1 = 45^\circ, \beta_2 = 45^\circ, \gamma_3 = 45^\circ$. (b) Reconstruction of a pair of straight lines for the data used in Figure 11(a) using a third projection. The projection of the pair of sequences obtained as solutions in Figure 11(a) are superimposed on the third projection of the pair of straight lines. This helps to identify the unique solution among the two possible solutions.

5 CONCLUSIONS

Discussions presented in this paper provide a methodology of finding an unique solution for the reconstruction of quadratic curves without the requirement of point to point correspondence, as well as constraint of transparency on the curve. The case of reconstruction of circles, parabolas and pair of straight lines in 3-D space are demonstrated in Figures 2 to 11.

References

- [1] Balasubramanian, R., Sukhendu Das and Swaminathan, K. (1999) Analytical formulations for the reconstruction of a line in 3-D space from two arbitrary perspective views, *Proc. of Satellite Conference on Image Analysis in Materials and Life Sciences*, IGCAR, Kalpakkam, India, Nov. 8–11, 1999, pp. 17–22.
- [2] Balasubramanian, R., Sukhendu Das and Swaminathan, K. (2000) Reconstruction of 3-D quadratic curves from arbitrary perspective views, *Proc. of the International Conference on Communications, Computers and Devices*, Vol. 2, I.I.T., Kharagpur, December 14–16, 2000, pp. 477–480.
- [3] Balasubramanian, R., Sukhendu Das and Swaminathan, K. (2000) Simulation studies for the performance analysis of the reconstruction of a line using stereoscopic projections, *Proc. of Indian Conference on Computer Vision, Graphics and Image Processing*, IISc, Bangalore, India, Dec. 20–22, 2000 pp. 338–344.
- [4] Balasubramanian, R., Sukhendu Das and Swaminathan, K. Error analysis in reconstruction of a line in 3-D from two arbitrary perspective views (accepted), *International Journal of Computer Mathematics* (Vol. 79(3 or 4)). U.K.: Gordon and Breach Publishing Group.
- [5] Brannan, D. A., Esplen, M. E. and Gray, J. J. (1999) *Geometry*, Cambridge University Press.
- [6] Kanatani, K. and Liu, W. (1993) 3-D interpretation of conics and orthogonality, *Computer Vision, Graphics and Image Processing* (Vol. 58), pp. 286–301.
- [7] Kahl, F. and Heyden, A. (1998) Using conic correspondences in two images to estimate the epipolar geometry, *Proceedings of International Conference on Computer Vision*, pp. 761–766.
- [8] Quan, L. (1996) Conic reconstruction and correspondence from two views, *IEEE Transactions on Pattern Analysis and Machine Intelligence* (Vol. 18, No. 2), pp. 151–160.
- [9] Rodriguez, J. J. and Aggarwal, J. K. (1988) Quantization error in stereo imaging, *CVPR*, pp. 153–188.
- [10] Safae-Rad, R., Tchou Kanov, I., Benhabib, B. and Smith, K. C. (1992) 3-D pose estimation from a quadratic curved feature in two perspective views, *Proc. 11th International Conference on Pattern Recognition*. The Hague, pp. 341–344.
- [11] Xie, M. and Thonnat, M. (1992) A theory of 3-D reconstruction of heterogenous edge primitives from two perspective views, *ECCV*, pp. 715–719.
- [12] Xie, M. (1994) On 3-D reconstruction strategy: A case of conics, *ICPR (A)*, pp. 665–667.